Random Gust Response Statistics for Coupled Torsion-Flapping Rotor Blade Vibrations

G. H. GAONKAR*
Southern University of Illinois, Edwardsville, Ill.
AND
K. H. HOHENEMSER† AND S. K. YIN‡
Washington University, St. Louis, Mo.

An analysis of coupled torsion-flapping rotor blade vibrations in response to atmospheric turbulence revealed that at high rotor advance ratios anticipated for future high speed pure or convertible rotorcraft both flapping and torsional vibrations can be severe. While appropriate feedback systems can alleviate flapping, they have little effect on torsion. Dynamic stability margins have also no substantial influence on dynamic torsion loads. The only effective means found to alleviate turbulence caused torsional vibrations and loads at high advance ratio was a substantial torsional stiffness margin with respect to local static torsional divergence of the retreating blade.

Nomenclature

$A(t)$	= state matrix
$A^T(t)$	= transpose of $A(t)$
$a = 2\mu/(L/R)$	= nondimensional turbulence parameter
B	= tip-loss factor
$C(t)$, $C_\delta(t)$,$C_{\theta_0}(t)$	= aerodynamic damping
c	= blade chord
$E[\ldots]$	= mathematical expectation of $[\ldots]$
$E[N_{+x_j}(\zeta,t)]$	= time variable expected number of positive crossings per unit time of threshold ζ for response component X_j
$F = (I_1/I_f)(c/4R)$	= nondimensional quantity
$f\Omega$	= blade torsional frequency
I	= identity matrix
I_1	= flapping mass moment of inertia
I_f	= feathering mass moment of inertia
$K(t)$,$K_\delta(t)$	= aerodynamic stiffness
K_f	= flapping feedback gain
K_0	= coning feedback gain
L	= scale of longitudinal turbulence
$1_{r\beta}(t)$,$1_{r\dot\beta}(t)$,$1_{r\theta_0}(t)$,$1_{r\lambda}(t)$	= aerodynamic lift, reversed flow region
$m_{\theta_0}(t)$,$m_{\theta_1}(t)$,$m_\lambda(t)$	= aerodynamic flapping moments
N	= number of blades per rotor
$n(t)$	= white noise input vector
$P\Omega$	= blade flapping frequency
$Q = (I_1/I_f)(C/4R)$	= nondimensional quantity
R	= rotor radius
$R_{xx}(t_1,t_2)$	= correlation matrix of $X(t)$
$R_{xx}(t,t) = P(t)$	= variance matrix of $X(t)$
t	= nondimensional time, time unit $1/\Omega$
V	= flight velocity
w	= vertical turbulence velocity
$X(t)$	= state or output vector
$X^T(t)$	= transpose of $X(t)$
β	= blade flapping angle
γ	= blade Lock inertia number
δ	= torsional elastic deflection from root to blade tip
$\delta(\ldots)$	= Dirac delta function
ζ	= response value exceeded in a threshold crossing
θ_0	= blade root pitch angle
$\lambda = w/\Omega R$	= nondimensional vertical turbulence velocity
$\mu = V/\Omega R$	= rotor advance ratio
ξ	= real part of characteristic value
$\sigma_{x_j}(t) = [R_{x_jx_j}(t)]^{1/2}$	= standard deviation of $x_j(t)$
σ_β	= standard deviation of β
σ_δ	= standard deviation of δ
τ	= nondimensional time, time unit $1/\Omega$
$\phi(t,\tau)$	= state transition matrix
Ω	= angular rotor speed

Received February 22, 1972; revision received June 14, 1972. Sponsored by the Ames Directorate, AAMRDL, under Contract NAS2-4151.
Index categories: VTOL Vibration; Structural Dynamic Analysis.
* Visiting Research Professor. Member AIAA.
† Professor of Aerospace Engineering. Associate Fellow AIAA.
‡ Post-doctoral Research Associate.

Introduction

THE problem of random rotor blade flapping vibrations caused by atmospheric turbulence has been studied earlier.[1] It was found that at high-rotor advance ratios anticipated for future high-speed pure or convertible rotorcraft, severe random vibrations and dynamic loads can occur, unless flapping or hub moment feedback systems are applied.[2] The blade representation used in these studies was a rigid straight blade flexibly attached at the rotor center, using quasi-steady linear aerodynamics including reversed flow effects but excluding nonuniform inflow, stall and compressibility effects.[3] Extensive wind-tunnel tests have shown that this representation gives useful approximations to the flapping response for low-lift high-advance ratio conditions, if the root flexibility is appropriately selected to represent the actual blade.[4] Even if the elastic center, the center of gravity and the aerodynamic center of the rotor blade cross section coincide, as they usually approximately do in practical blade designs, large blade torsional moments occur in the region of reversed flow, because the aerodynamic center is then shifted from the quarter chord point to the three quarter chord point.[5] It is, therefore, of interest to study the effects of atmospheric turbulence on the coupled torsion-flapping rotor blade vibrations.

Blade Representation and Method of Analysis

It is assumed that the blade torsion mode is a straight line through the rotor center, that in regions of normal flow direction the aerodynamic center, the center of gravity and the shear center of blade cross section coincide, and that linear quasi-static aerodynamics are used. Because of the higher frequency of the torsional vibrations the last assumption is more questionable than for the flapping case and as yet no tests are available to substantiate the analysis of Ref. 5.

Though quantitatively the results to be presented here may require some corrections due to over simplified aerodynamic assumptions the established important trends should remain valid, if reversed flow stall flutter is avoided.[6]

When the dynamic equations of blade flapping and blade torsion, given in Ref. (5), are extended to include the effect of root pitch angle θ_0, one obtains

$$(2/\gamma)\ddot{\beta} + C(t)\dot{\beta} + [(2P^2/\gamma) + K(t)]\beta - m_{\theta_1}(t)\delta = m_\lambda(t)\lambda + m_{\theta 0}(t)\theta_0 \quad (1)$$

$$(1/3\gamma)\ddot{\delta} + FC_\delta(t)\dot{\delta} + [(f^2/3\gamma) + QK_\delta(t)]\delta + Ql_{r\dot{\beta}}(t)\dot{\beta} + Ql_{r\beta}(t)\beta + (1/2\gamma)\ddot{\theta}_0 + FC_{\theta 0}(t)\dot{\theta}_0 = -Q[l_{r\lambda}(t)\lambda + l_{r\theta 0}(t)\theta_0] \quad (2)$$

The flapping feedback is assumed to occur without producing a mechanical flapping moment. The only periodic coefficient not defined in either Ref. (3) or (5) is $l_{r\theta 0}$ with the value in the normal flow region,

$$1_{r\theta 0} = 0$$

$$1_{r\theta 0} = \mu^4[-(1/32) + (1/24)\cos 2t - (1/96)\cos 4t]$$

in the mixed flow region, and

$$1_{r\theta 0} = -[(B^4/4) + (B^2\mu^4/4)] - (2/3)B^3\mu \sin t + (B^2\mu^2/4)\cos 2t$$

in the reversed flow region.

For the blade without feedback, $\theta_0 = 0$. In case of pitch-flap coupling, θ_0 is to be replaced by

$$\theta_0 = -K_f\beta \quad (3a)$$

In case of coning angle feedback, θ_0 is to be replaced by

$$\theta_0 = -K_0\left((1/N)\sum_{K=1}^{N}\beta_k\right) \quad (3b)$$

where all blades are assumed to perform the same flapping motion except for appropriate phase shifts.

In order to obtain from Eqs. (1–3) the response to the random vertical gust velocity λ, it is assumed that this gust velocity at a point in time is uniformly distributed over the rotor disk, an assumption which has been proven approximately valid for current ratios of turbulence scale L over rotor radius R.[7] If one approximates the widely used von Kármán–Taylor turbulence spectrum by one with exponential autocorrelation function,[1] the dimensionless vertical turbulence velocity λ is determined from[7,8]

$$\dot{\lambda} + a\lambda = \sigma_\lambda(2a)^{1/2}n(t) \quad (4)$$

where $n(t)$ has the autocorrelation function

$$R_n(\tau) = \delta(\tau) \quad (5)$$

We now express the dynamic Eq. (1–4) in state variable form

$$\dot{X}(t) = A(t)X(t) + B(t)n(t) \quad (6)$$

The response variance $P(t)$ can then be determined from the matrix equation[8–10]

$$\dot{P}(t) = A(t)P(t) + P(t)A^T(t) + B(t)B^T(t) \quad (7)$$

with zero initial state, and the response covariance matrix is obtained from

$$\begin{aligned} R_{xx}(t_1,t_2) &= \phi(t_1,t_2)P(t_2) && \text{for } t_1 \geqslant t_2 \\ &= P(t_1)\phi^T(t_2,t_1) && \text{for } t_1 \leqslant t_2 \end{aligned} \quad (8)$$

where the state transition matrix is defined by

$$\dot{\phi}(t,\tau) = A(t)\phi(t,\tau),\ \phi(\tau,\tau) = I \quad (9)$$

Once the response covariance matrix is known, the threshold crossing expectations can be determined from expressions given in the literature.[7]

For an alternative method[1] the covariance matrix is

$$R_{xx}(t_1,t_2) = \int_{-\infty}^{\infty} H^*(\omega,t_1)S_\lambda(\omega)H^T(\omega,t_2)d\omega \quad (10)$$

with

$$S_\lambda(\omega)/\sigma_\lambda^2 = a/\pi(a^2 + \omega^2) \quad (11)$$

and $H(\omega,t)$ the response vector to the input $\lambda(t) = u(t)\exp i\omega t$, $u(t)$ being the unit step function. The numerical examples were computed with the second method, truncating $S_\lambda(\omega)$ at $|\omega| > 3$. The first method gives slightly different results with about one third the computational effort.

Numerical Results

As before,[1] the numerical data are for a lifting rotor operating with a rotor advance ratio of $\mu = 1.6$, which corresponds at a flight speed of 280 knots to a blade tip speed of $\Omega R = 300$ fps. In the stochastic analysis the standard deviation of the dimensionless vertical turbulence velocity $\lambda = w/\Omega R$ is assumed to be $\sigma_\lambda = 1$, which results in Eq. (4). 8 fps is a representative value[1] for the standard deviation of the vertical turbulence velocity, occurring at low altitudes with 0.1% probability. Using this value and $\Omega R = 300$ fps we have $\sigma_\lambda = 1.5°$. The nondimensional standard deviations σ_β, σ_δ for flapping and elastic blade twist, respectively, and the thresholds ζ shown in the figures must then be multiplied by 1.5 to obtain the dimensional values of these quantities in degrees. The remaining rotor parameters are also the same as before[1]: Tip loss factor $B = 0.97$, Lock number $\gamma = 4$ and turbulence scale over rotor radius $L/R = 12$, which corresponds for a rotor radius of 33 ft to 400 ft turbulence scale length, typical of low altitude turbulence. The flapping frequency ratio is assumed as $P = 1.3$. Further assumed is a flapping over feathering inertia ratio of $I_1/I_f = 940$ and a radius over blade chord ratio of 15.6, resulting in $F = 0.24$ and $Q = 15$. The torsional blade frequency is assumed to vary between $f = 8$ and $f = 12$. In addition to the response data of Figs. 3–8 dynamic stability data for the blade are shown in Figs. 1 and 2. These figures give the real part ξ of the characteristic values of the Floquet state transition matrix[2] vs pitch-flap coupling gain K_f. The curves indicated by crosses represent conjugate complex characteristic values; the curves indicated by circles represent a single characteristic value. Figure 1 is for $f = 8$. The blade is very stable (negative ξ) up to about $K_f = 0.5$, has a minimum of stability of about $K_f = 1.5$, reaches a relative stability maximum of $K_f = 2.0$ and becomes unstable at $K_f = 2.4$. Figure 2 is for $f = 10$. The stability is almost unchanged up to $K_f = 0.5$ and at $K_f = 2.0$, but is improved at $K_f = 1.5$, and the stability

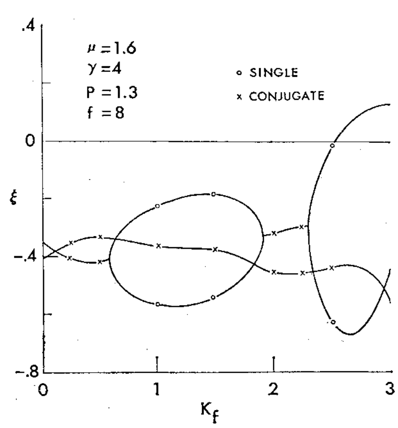

Fig. 1 Real part ξ of characteristic value vs flapping feedback gain K_f, $f = 8$.

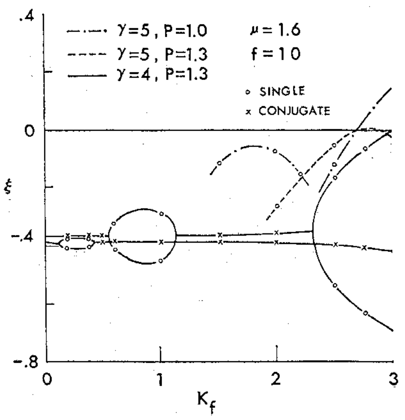

Fig. 2 Real part ξ of characteristic value vs flapping feedback gain K_f, $f = 10$.

limit is raised to $K_f = 3.0$. The dash-dash line indicates that an increase in Lock number is destabilizing, the dash-dot line indicates that for a pure flapping blade without elastic flapping restraint ($P = 1$) the blade reaches almost its stability limit at $K_f = 1.7$.

Figures 3 and 4 show the time variable standard deviations of the basic blade with torsional frequency ratio $f = 8$ for zero feedback, for flapping feedback with $K_f = 0.4$ and for coning angle feedback with $K_0 = 0.4$. The flapping maximum standard deviation is reduced by either of the feedbacks from 2.3 to 1.5, the torsion maximum standard deviation is very high—about 6—and not much affected by feedback. The figures show the second revolution after imposing the turbulence excitation, when the response standard deviations are almost stabilized and periodic. The blade is in the aft position at $t = 0$, 2π, 4π, etc. The maximum flapping standard deviation occurs when the blade is approximately in the forward position, the maximum torsion standard deviation occurs, when the blade is in the region of maximum reversed flow.

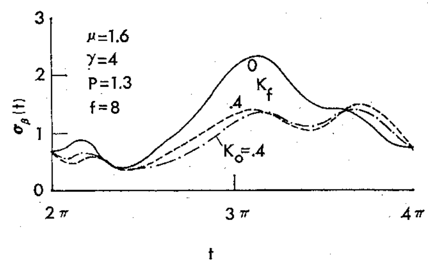

Fig. 3 Flapping standard deviation $\sigma_\beta(t)$ for zero feedback, $K_f = 0.4$ and $K_0 = 0.4$, $f = 8$.

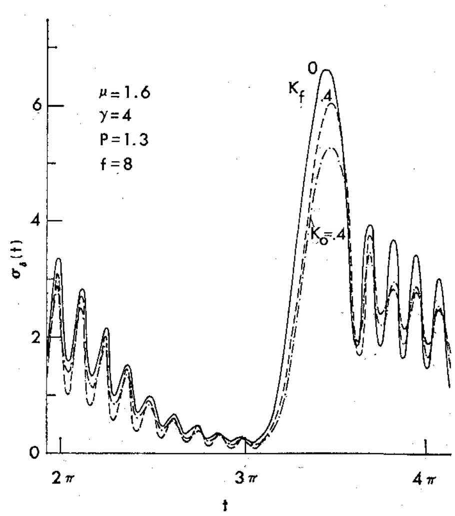

Fig. 4 Torsion standard deviation $\sigma_\delta(t)$ for zero feedback, $K_f = 0.4$ and $K_0 = 0.4$, $f = 8$.

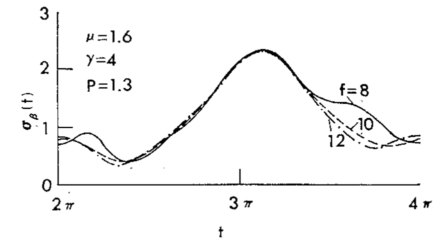

Fig. 5 Flapping standard deviation $\sigma_\beta(t)$ for $f = 8$, 10, 12; no feedback.

Figures 5 and 6 show for the basic blade without feedback the effect of torsional frequency ratio f on the standard deviations. From Fig. 5 it is seen that flapping is little affected by a variation in f. Figure 6 shows a very large effect of f on the torsional standard deviation, much more than would be expected from the increase in torsional stiffness. For example this increase would account for a reduction factor of 0.64 when changing from $f = 8$ to $f = 10$. The actual reduction factor for the maximum standard deviation is 0.37. It was found that for constant feathering moment of inertia the blade experiences static torsional divergence in the reversed flow region at $f = 6.6$. Though dynamic instability would not occur at $f = 6.6$, the torsional deflections would be extremely high. The closeness to the static torsional divergence limit is presumably the reason why an increase in torsional stiffness from $f = 8$ to $f = 10$ causes a decrease in torsional maximum standard deviation substantially larger than normally expected from the torsional stiffness increase, see also the discussion of Fig. 21 in Ref. 11.

Figure 7 shows the responses β and δ of the basic blade with $f = 10$ to a step gust input $\lambda = 1$ at $t = 0$, when the blade is in the aft position. The dash line is obtained when the coupling terms in Eqs. (1) and (2) are omitted. Flapping is hardly affected, however, the torsional response is much reduced without the coupling terms. While qualitatively the torsional response to turbulence could be studied without coupling with flapping, the results would be quite unconservative.

Figures 8 and 9 show the expected number of upcrossings per unit of time of the positive levels $\zeta = 2$ and $\zeta = 3$ for

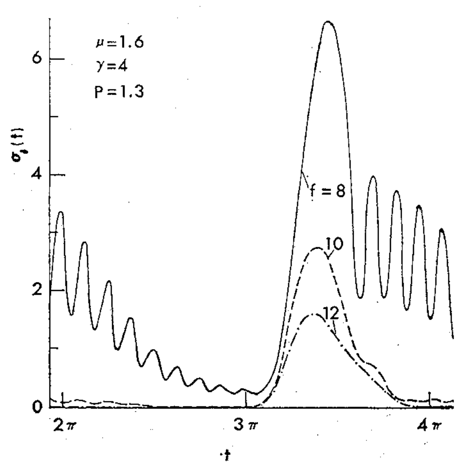

Fig. 6 Torsion standard deviation $\sigma_\delta(t)$ for $f = 8$, 10, 12; no feedback.

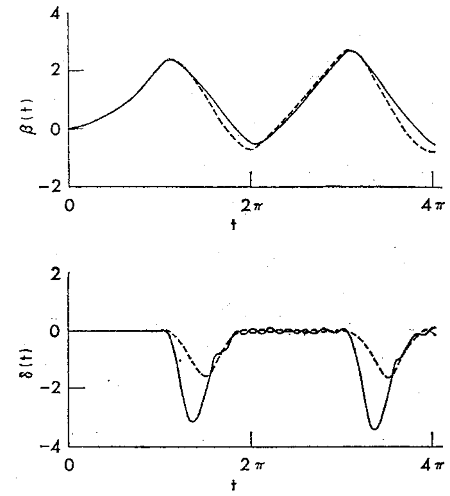

Fig. 7 Flapping and torsion response $\beta(t)$, $\delta(t)$ for unit gust input (dash lines: no torsion-flapping coupling).

flapping and torsion, respectively. The solid lines are for $f = 10$, the dash lines for $f = 8$. Note for torsion the very large reduction in the number of crossings when changing from $f = 8$ to $f = 10$ (Fig. 9), while this change hardly affects the number of crossings for flapping (Fig. 8).

Unlike the configuration $f = 8$, the torsionally stiffer blade with $f = 10$ shows upcrossings of the levels $\zeta = 2$ and 3 only within a short time period of the order of the period of the natural torsional mode. One can, therefore conclude that in most cases an upcrossing will lead to a single peak value within a revolution. The number of peaks per revolution above the level ζ can then be approximated by integrating the curves of Fig. 9 over one revolution. This method is not applicable at the shown ζ levels for $f = 8$. For flapping with its natural period close to 2π this method of obtaining the number of peaks per revolution exceeding the level $\zeta = 2$ or $\zeta = 3$ is justified both for $f = 8$ and $f = 10$, as is seen from Fig. 8. The crossing expectations for the levels $\zeta = -2$ and $\zeta = -3$ are similar to those shown in Figs. 8 and 9, except that the curves are somewhat shifted on the time scale.

The case of $f = 10$ and an advance ratio of $\mu = 0.8$ has also been computed. In this case the torsion response is quite small, since the torsional divergence limit is reduced from $f = 6.6$ to $f = 1.4$, so that a very large torsional stiffness margin exists.

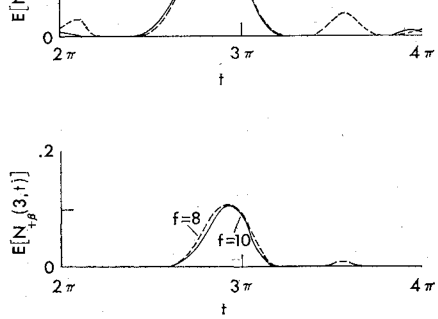

Fig. 8 Expected number of flapping upcrossings per unit time of levels $\zeta = 2$ and $\zeta = 3$; no feedback.

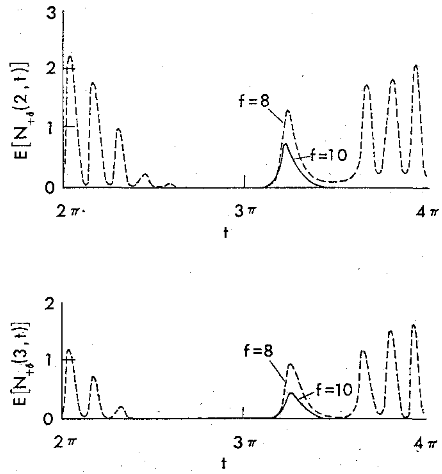

Fig. 9 Expected number of torsion upcrossings per unit time of levels $\zeta = 2$ and $\zeta = 3$; no feedback.

Conclusion

In summary, it can be concluded from the numerical examples that blade torsional response to atmospheric turbulence at high rotor advance ratio ($\mu = 1.6$) can be very severe unless the torsional blade stiffness is several times greater than that for the static torsional divergence limit in the region of maximum reversed flow. Flapping-torsion coupling has little effect on flapping but has a large detrimental effect on torsion. The preceding analysis of blade responses to atmospheric turbulence is for rigid rotor support omitting higher blade modes. The effects of elastic rotor supports, of second mode blade bending and of random rotorcraft motions due to turbulence remain to be determined.

References

[1] Gaonkar, G. H. and Hohenemser, K. H., "Stochastic Properties of Turbulence Excited Rotor Blade Vibrations," *AIAA Journal*, Vol. 9, No. 3, March 1971, pp. 419–424.

[2] Yin, S. K. and Hohenemser, K. H., "The Method of Multiblade Coordinates in the Linear Analysis of Lifting Rotor Dynamic Stability and Gust Response," Paper 512, *27th Annual National Forum of the American Helicopter Society*, May 1971.

[3] Sissingh, G. J., "Dynamics of Rotors Operating at High Advance Ratios," *Journal American Helicopter Society*, Vol. 13, No. 3, July 1968, pp. 56–63.

[4] Kuczynski, W. A., Sharpe, D. L. and Sissingh, G. J., "Hingeless Rotor-Experimental Frequency Response and Dynamic Characteristics with Hub Moment Feedback Controls," Paper 612, *28th Annual National Forum of the American Helicopter Society*, May 1972.

[5] Sissingh, G. J. and Kuczynski, W. A., "Investigation on the Effects of Torsion on the Dynamics of the Flapping Motion," *Journal of American Helicopter Society*, Vol. 15, No. 2, April 1970, pp. 2–9.

[6] White, R. P., Jr., "Instabilities Associated with a Rotor Blade Stopped in Flight," Paper 229, *24th Annual Forum of the American Helicopter Society*, May 1968.

[7] Gaonkar, G. H. and Hohenemser, K. H., "An Advanced Stochastic Model for Threshold Crossing Studies of Rotor Blade Vibrations," *AIAA Journal*, Vol. 10, No. 8, Aug. 1972, to be published.

[8] Wan, F. Y. M. and Lakshmikantham, C., "Rotor Blade Response to Random Loading: A Direct Time Domain Approach," AIAA Paper 72-169, San Diego, Calif, 1972.

[9] Van Trees, H. L., *Detection, Estimation and Modulation Theory*, Wiley, New York, 1968.

[10] Gaonkar, G. H., "Interpolation of Aerodynamic Damping of Lifting Rotors in Forward Flight from Measured Response Variance," *Journal of Sound and Vibrations*, Vol. 18, No. 3, 1971, pp. 381–389.

[11] Wachs, M. A. and Rabbott, J. P., Jr., "Rotary Wing Aircraft Design Trends," *Journal of American Helicopter Society*, Vol. 9, No. 2, April 1964, pp. 1–16.